

# An estimate of the circulation generated by a bluff body

T. S. Morton<sup>\*</sup>

---

## Abstract

A loss in circulation is sometimes cited in connection with bluff-body wakes as a result of comparing a well-known theoretical estimate of the total circulation generated by a cylinder with the circulation actually observed downstream. In an effort to better understand this reported loss in circulation, an alternative estimate of the circulation generated by a cylinder is derived by integrating the velocity on a closed loop containing the attached boundary layer. Predictions of the dimensionless circulation are less than the previous theoretical estimate and comparable to observed values, regardless of the velocity profile assumed at the point of separation. This suggests that the total circulation generated by bluff bodies may have been overestimated in the past, and that comparison of observed values with this overestimate is the origin of the perceived “loss” in circulation.

Keywords: Wake, circulation, bluff-body, cylinder

---

## 1. Introduction

The purpose of this study is to provide an estimate of the mean circulation generated by a bluff body in steady motion through a fluid. This circulation has been estimated by considering it to be generated at a rate of  $(1 - C_{pb})v_\infty^2/2$  per shedding period [1]. Here,  $C_{pb}$  is the base pressure coefficient, and  $v_\infty$  is the free stream velocity. The following dimensionless form of this estimate was later used in a study of square section cylinders [2]:

$$\frac{\Gamma}{Dv_\infty} = \frac{(1 - C_{pb})}{2St}, \quad (1)$$

where  $\Gamma$  is the total circulation generated by the body, and  $D$  is the body dimension. This estimate predicts a total circulation of more than twice that typically found in bluff-body wakes, and it is generally believed that half or more of the vorticity is cancelled in the near wake due to mixing [2]. The fact that Fage and Johansen [3] were only able to account for roughly 60% of the total vorticity nine body lengths downstream, which led them to first suggest the mixing of positive and negative vorticity in the wake, appears to be the origin of the justification of Eq. (1). They later [4] made detailed graphical estimates in the near wake, however, and appear to have adequately accounted for the total vorticity to within 10% error. Subsequent studies have shown that only 35~45% of the total vorticity predicted by Eq. (1) can be found in the near wake [5, 6]. Davies [7] found that only 26% of the vorticity predicted by Eq. (1) is found in the wake of a D-shaped cylinder 8 diameters downstream. Wu *et al.* [8] reported a value of  $\Gamma_{KM}/(Dv_\infty) = 3.5$  for the mean circulation of Kármán vortices behind a cylinder at  $Re = 525$ . Likewise, in the range  $73 \leq Re \leq 226$ , a comparable value of  $\Gamma_{KM}/(\pi Dv_\infty) \approx 1$  is observed in the cylinder wake [9]. At  $Re = 1.44 \times 10^5$ , the circulation in the wake of a cylinder has been found to be  $\Gamma/Dv_\infty = 2.6$  [5],

---

<sup>\*</sup> inquiries@mortonresearch.org

whereas Eq. (1) gave an estimate of  $\Gamma/Dv_\infty = 5.86$ . The total dimensionless circulation of a rectangular cylinder with a blunt leading edge was likewise found to be approximately 2.0 [10]. In a computational study of the unsteady wake of a disk, Johari and Stein [11] obtained a value of  $\Gamma/(Dv_\infty) = 2.6$ , which compares well with the experimental value of  $\Gamma/(Dv_\infty) = 2.5$  [12].

The anomalous mixing of positive and negative vorticity has been characterized as “a long standing puzzle” [13]. In what follows, a simple estimate of the dimensionless circulation will be derived using a contour integration that includes the attached boundary layer on a circular cylinder in cross flow. Predictions are significantly lower than those of Eq. (1) and agree fairly well with values cited above. In particular, it can be seen that regardless of the velocity profile from the point of separation, the dimensionless circulation generated up to the point of separation is near 2.0 for a circular cylinder. Consequently, the “anomalous mixing” argument is not required in order to reconcile the present estimation method with the circulation observed in wakes.

## 2. Cylinder Wake Circulation

Due to the no slip condition of the attached boundary layer, a bluff body such as a circular cylinder transmits a torque to the fluid passing it. This torque sets some region of the fluid in motion rotationally. The resulting circulation can be determined by performing the following contour integration

$$\Gamma_{(1/2)} = \oint v \cdot ds \quad (2)$$

along the loop  $\gamma_1 + \gamma_2 + \gamma_3 + \gamma_4$  shown in Figure 1. The subscript “(1/2)” in Eq. (2) indicates that this represents only half of the total circulation generated by a symmetric mean flow about the cylinder. The contour integration is performed in 4 parts. On the curve  $\gamma_1$  (see Figure 1), the approaching fluid decelerates and stagnates according to the velocity distribution for ideal fluid flow past a cylinder ( $n = 2$ ) or a sphere ( $n = 3$ ). Along  $\gamma_2$ , which terminates at the separation point, the velocity is zero due to the no-slip condition.

The time-mean velocity on the contour  $\gamma_3$ , which emanates from the separation point, is assumed to be entirely in the free-stream direction, as shown in Figure 1, and modeled by a function such as the following:

$$\frac{v}{v_\infty} = \left(1 - e^{k(a-r)}\right) + c_1 \frac{(r-a)^q}{c_2 + (r-a)^m}. \quad (3)$$

The middle term handles the no-slip condition by bringing the velocity from 0 at the body to 1 at infinity. The term on the right gives the well-known bulge to the velocity profile (see Figure 2). Here,  $a$  is the radius of the cylinder, and the constants  $c_1$ ,  $c_2$ ,  $q$ , and  $m$  are all positive. This “peak” term on the right side of Eq. (3) has more flexibility to fit velocity profile data than, for example, the vortex of Oseen [14] which, if modified for the presence of a body, would be:

$$v_\theta = \frac{c}{(r-a)} \left(1 - e^{-\left(\frac{r-a}{a}\right)^2}\right). \quad (4)$$

Since the direction of  $v$  in Eq. (3) is parallel to the free stream (see Figure 1), the velocity component in the direction of  $\gamma_3$  can be obtained by multiplying Eq. (3) by  $\cos\theta$ , where  $\theta$  is the separation angle. The

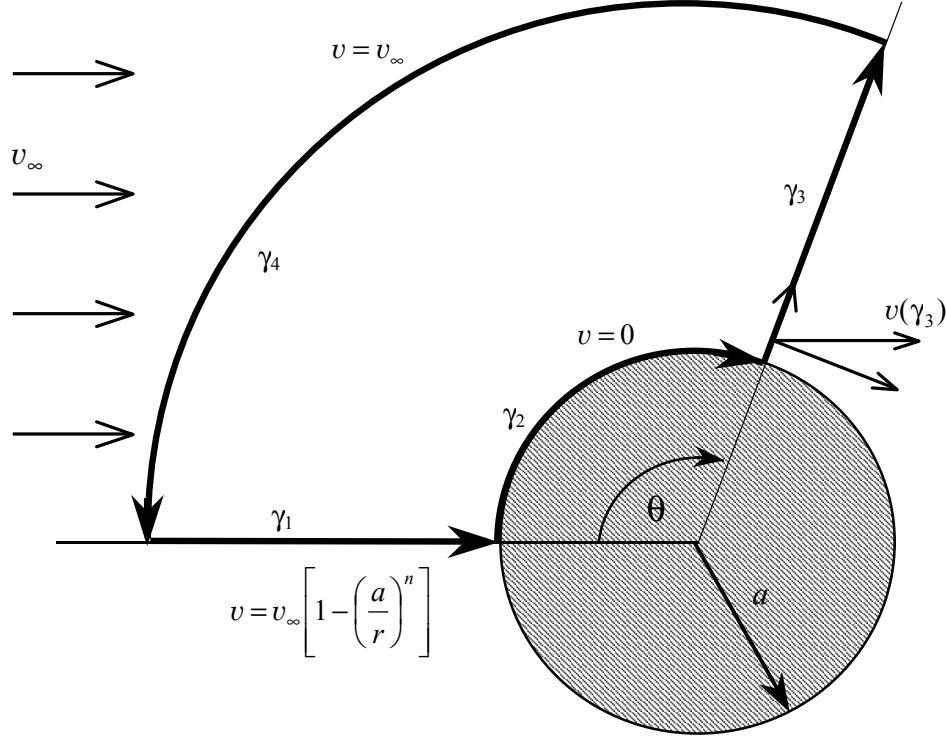


Figure 1. Schematic of integration contour for computing circulation.

distance from the center of the cylinder to the contour  $\gamma_4$  will be denoted by  $r_\infty$ . On this contour, the magnitude of the velocity is  $v_\infty$ , so its component in the direction along the contour  $\gamma_4$  is  $-v_\infty \sin \varphi$ , where  $\varphi$  is the angle (measured from the same direction from which  $\theta$  is measured) required to reach a given point on the contour  $\gamma_4$ .

Referring to Figure 1, the integration in Eq. (2) is now rewritten piecewise:

$$\frac{\Gamma_{(1/2)}}{v_\infty} = \int_{r_\infty}^a \left[ 1 - \left( \frac{a}{r} \right)^n \right] dr + \cos \theta \int_a^{r_\infty} \left[ \left( 1 - e^{k(a-r)} \right) + \frac{c_1 (r-a)^q}{c_2 + (r-a)^m} \right] dr - \int_\theta^0 \sin \varphi r_\infty d\varphi$$

All but one of the terms can be integrated easily, giving:

$$\frac{\Gamma_{(1/2)}}{v_\infty} = \frac{na}{n-1} - \frac{a^n r_\infty^{1-n}}{n-1} + \left( \frac{e^{k(a-r_\infty)}}{k} - \frac{1}{k} - a \right) \cos \theta + \cos \theta \int_a^{r_\infty} \frac{c_1 (r-a)^q}{c_2 + (r-a)^m} dr$$

after canceling terms containing  $r_\infty$ .

Taking the limit as  $r_\infty \rightarrow \infty$ , with  $n > 1$ ,  $\Gamma = 2\Gamma_{(1/2)}$ , and  $a = D/2$  gives:

$$\frac{\Gamma}{Dv_\infty} = \frac{n}{n-1} - \left( 1 + \frac{1}{ka} \right) \cos \theta + \frac{\cos \theta}{a} \int_a^{r_\infty} \frac{c_1 (r-a)^q}{c_2 + (r-a)^m} dr. \quad (5)$$

Making the substitution  $w = c_2 + (r-a)^m$  in the integral above shows that it is unbounded if  $m - q \leq 1$ . Incidentally, when  $q=1$  and  $m=2$ , the integrand is a generalization of the vortex studied by Scully and

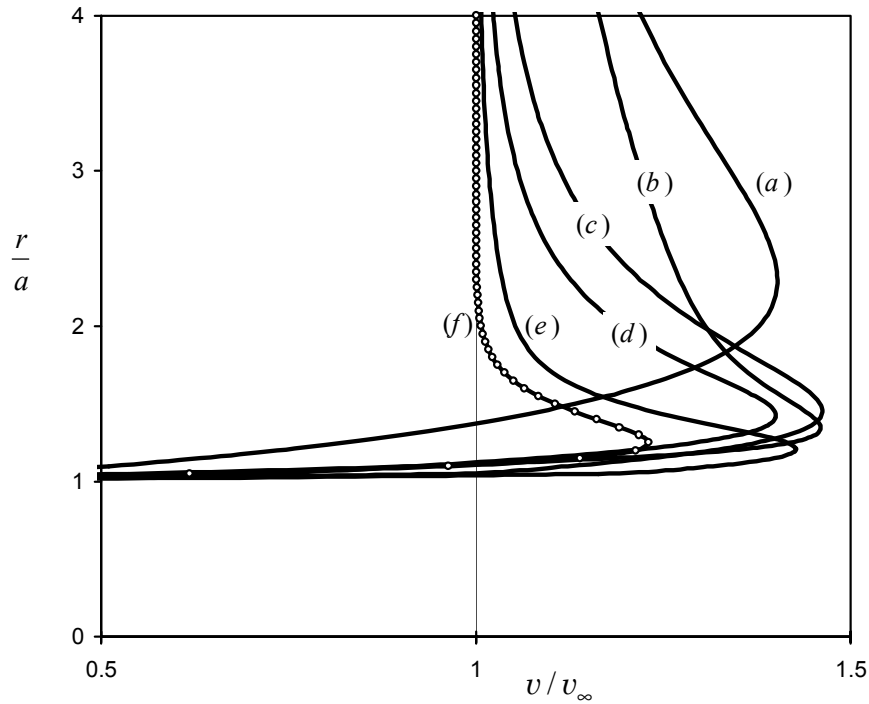


Figure 2. Velocity profiles on  $\gamma_3$  for various sets of curve-fitting parameters. Labels refer to case headings in Table 1.

Sullivan [15] (see also [16]). When the separation angle is  $\theta = \pi/2$ , the dimensionless circulation is simply the first term on the right side of (5), namely  $n/(n-1)$ . This can also be seen by noting that the integral of the velocity along  $\gamma_3$  is zero in such cases. For  $\theta = \pi/2$ , therefore, the dimensionless circulation is 2 for a circular cylinder and 3/2 for a sphere, regardless of the fit chosen for the velocity profile on the contour  $\gamma_3$ . Figure 2 shows a wide range of possible velocity profiles on  $\gamma_3$ , and Table 1 shows the curve-fitting constants used to obtain these curves. Figure 3 illustrates the range of values predicted by Eq. (5) for the various velocity profiles shown in Figure 2. Here, the final term in Eq. (5) is integrated numerically. An alternative to the peaking function in Eq. (3) that appears to be as adaptable as Eq. (3) in the region of interest is contained in the following:

$$\frac{v}{v_\infty} = \left(1 - e^{k(a-r)}\right) + \frac{c_1(r-a)}{1 + c_2 e^{m(r-a)}}. \quad (6)$$

Although series representations exist for the integral of the term on the right in Eq. (6), it is simpler to integrate numerically. Furthermore, the integral is simple enough that its behavior can be represented adequately by the following function:

$$\int_0^\infty \frac{x}{1 + c_2 e^{mx}} dx = \frac{1}{m^2 (c_2 + 0.245 c_2^{0.267})}. \quad (7)$$

Case (f) in Table 1 employs Eq. (6) instead of Eq. (3) for the velocity profile on  $\gamma_3$ .

	Case (a)	Case (b)	Case (c)	Case (d)	Case (e)	Case (f)
Eq. for $\gamma_3$ :	(3),(5)	(3),(5)	(3),(5)	(3),(5)	(3),(5)	(6),(7)
$k$	0.2208	1.5697	2.698	3	3	10
$c_1$	4.2576	0.5546	0.5611	0.3042	0.1113	30
$c_2$	2.6104	0.079	0.5207	0.2487	0.0851	7
$q$	0.5213	0.897	0.08	0.2651	0.08	–
$m$	1.8518	1.947	2.1965	2.6	2.6	4

Table 1. Curve-fitting constants for cases plotted in Figure 2 and Figure 3.

Each point of a given curve in Figure 3 corresponds to a separation point on the cylinder, from which the velocity profile is assumed to emanate. However, the velocity profile is not assumed to also emanate from all points on  $\gamma_2$  upstream of the separation point; therefore, the trend of a given curve in Figure 3 cannot be taken to represent the accumulation of circulation with the distance traveled along  $\gamma_2$ .

It appears, from Figure 3, that for most typical velocity profiles and separation angles, the predicted dimensionless circulation lies in the range:

$$1 < \frac{\Gamma}{Dv_\infty} < 3. \quad (8)$$

For an  $80^\circ$  separation angle, for example, if one makes the very reasonable requirement that the velocity profile decrease from some maximum to a value no greater than  $1.5v_\infty$  within one diameter of either side of the cylinder and to a value no greater than  $1.2v_\infty$  within 4 diameters of either side of the cylinder, then the upper bound in Eq. (8) certainly holds, regardless of the values chosen for the curve-fitting constants.

At the point of separation on the surface, the tangential velocity should obey the relation [17, p. 132]:

$$\left( \frac{\partial v}{\partial r} \right)_{r=0} = 0. \quad (9)$$

This effect is not modeled by the velocity profiles used in this study; however, its contribution to the integrals in (5) and (7) is very small owing to the smallness of the region that it affects.

In summary, the values predicted by Eq. (2), implemented herein by Eq. (5), are considerably smaller than those predicted by Eq. (1). This may help explain the “loss” in circulation sometimes referred to when using Eq. (1). In particular, the closer agreement with observed values suggests that this anomalous loss does not occur. Application of the method to a normal flat plate is particularly simple because there the separation point is known. The velocity upstream of the forward stagnation point in that case can be taken from Kirchhoff’s solution to the normal flat plate.

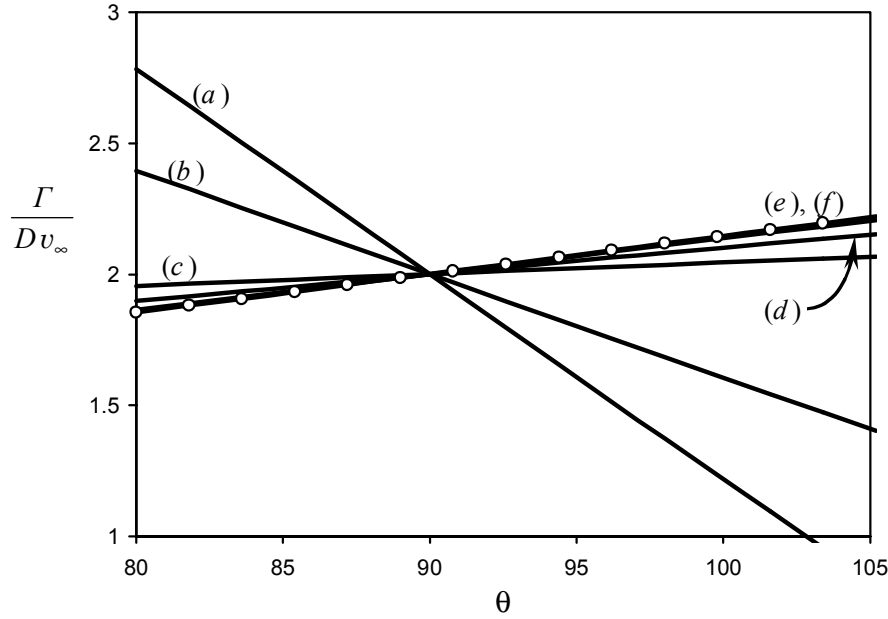


Figure 3. Dimensionless circulation vs. separation angle of a cylinder wake based on various possible curve fits of the velocity profile along  $\gamma_3$ . Labels refer to case headings in Table 1. All curve fits must pass through 2.0 for a separation angle of  $\theta = \pi/2$  due to the assumption of ideal 2D stagnation flow at the leading edge.

### 3. Conclusion

An estimate of the total circulation generated by a circular cylinder is derived by integrating the velocity on a loop containing the attached boundary layer up to the point of separation. The estimate is weakly dependent upon the velocity downstream of separation. For a separation angle of  $\theta = \pi/2$ , the prediction is independent of this downstream velocity, being  $\Gamma/(Dv_\infty) = 2$  when the approach velocity is modeled by ideal flow about a cylinder (in which case the velocity exponent is  $n = 2$ ). The method, which is based on the assumption that circulation is generated only by the attached boundary layer, gives estimates that are closer to observed values than previous estimates. Consequently, “anomalous mixing” is not required in order to reconcile the present estimation method with the circulation observed in wakes.

### References

- [1] Roshko, A., On the drag and shedding frequency of bluff cylinders. *NACA Technical Note* 3169 (1954).
- [2] Bearman, P. W. & Obasaju, E. D., An experimental study of pressure fluctuations on fixed and oscillating square-section cylinders. *Journal of Fluid Mechanics* **119**, pp. 297-321 (1982).
- [3] Fage, A. & Johansen, F. C., On the Flow of Air behind an Inclined Flat Plate of Infinite Span. *Proceedings of the Royal Society of London A* **116**, pp. 170-197 (1927).
- [4] Fage, A. & Johansen, F. C., The structure of the vortex street. *Philosophical Magazine* **5**, pp. 417-441 (1928).
- [5] Cantwell, B. J. & Coles, D., An experimental study of entrainment and transport in the turbulent near wake of a circular cylinder. *Journal of Fluid Mechanics* **136**, pp. 321-374 (1983).

- [6] Lyn, D. A., Einav, S., Rodi, W., & Park, J.-H., A laser-Doppler velocimetry study of ensemble-averaged characteristics of the turbulent near wake of a square cylinder. *Journal of Fluid Mechanics* **304**, pp. 285-319 (1995).
- [7] Davies, M. E., A comparison of the wake structure of a stationary and oscillating bluff body, using a conditional averaging technique. *Journal of Fluid Mechanics* **75**, pp. 209-231 (1976).
- [8] Wu, J., Sheridan, J., Hourigan, K., Welsh, M. C., & Thompson, M., Longitudinal vortex structures in a cylinder wake. *Physics of Fluids* **6**, pp. 2883-2885 (1994).
- [9] Green, R. B. & Gerrard, J. H., Vorticity measurements in the near wake of a circular cylinder at low Reynolds numbers. *Journal of Fluid Mechanics* **246**, pp. 675-691 (1993).
- [10] Wood, C. J., Visualizations of an incompressible wake with base bleed. *Journal of Fluid Mechanics* **29**, pp. 259-273 (1967).
- [11] Johari, H. & Stein, K., Near wake of an impulsively started disk. *Physics of Fluids* **14**, pp. 3459-3474 (2002).
- [12] Balligand, H., Unsteady wake structure behind a solid disk. Ph.D. Dissertation, Syracuse University (2000).
- [13] Zdravkovich, M., Comment on the Loss of Vorticity in the Near Wake of Bluff Bodies. *ASME Journal of Fluids Engineering* **111**, pp. 104-105 (1989).
- [14] Oseen, C. W., Über Wirbelbewegung in Einer Reibenden Flüssigkeit. *Ark. J. Mat. Astrom. Fys.* **7**, pp. 14-21 (1912).
- [15] Scully, M. P. & Sullivan, J. P., Helicopter Rotor Wake Geometry and Airloads and Development of Laser Doppler Velocimeter for Use in Helicopter Rotor Wakes. *MIT Aerophysics Laboratory Technical Report 183, MIT DSR No. 73032* (1972).
- [16] Scully, M. P., Computation of Helicopter Rotor Wake Geometry and Its Influence on Rotor Harmonic Airloads. *MIT Report No. TR 178-1* (1975).
- [17] Schlichting, H., *Boundary-Layer Theory*, McGraw-Hill, NY (1979).